The IRM Quarterly
Summer 2004, Vol. 14, No. 2

Mössbauer Revisited Again

measurement in applied fields

Thelma S. Berquó
Peat Sølheid
IRM

The use of Mössbauer spectroscopy as a complementary technique for the characterization of environmental systems (*i.e.* soils, iron oxides and oxyhydroxides) continues to grow: many papers are published each year and different samples have been the object of study. With application to an increasing variety of materials, new problems are emerging and additional tools are necessary. Here we will introduce another approach for taking Mössbauer spectra, using applied magnetic fields. Basic information on Mössbauer spectroscopy and regular spectra acquisition techniques were presented in two previous issues of *The IRM Quarterly* (Hunt, 1992; Solheid, 1998) and in the *MAG-NET MAGazine* (Muxworthy, 2000); a comprehensive reference is the book by Greenwood & Gibb (1972).

The basic Mössbauer experimental setup consists of a source mounted on a constant linear acceleration motor, an absorber (Mössbauer lingo for the sample), a sealed gas proportional counter and some lead shielding. To add experimental flexibility, the sample can be loaded into a cryostat with mylar access windows to permit the gamma-ray beam to be projected through the sample and into the counter. High-field spectrometers may apply a magnetic field parallel to the gamma beam (the source being positioned in the cryostat along with the sample), or a perpendicular field may be applied by a split coil (the source being mounted on one side of the cryostat tail, the counter on the other, and only the sample in the cryostat). The latter setup eliminates the need to handle the source each time the sample is changed and allows the motor to be fixed in place with a short drive shaft. At IRM we have the latter setup, a spectrometer with cryogenic dewar where we can study samples from liquid helium temperature (4.2 K) up to 300 K. Our dewar has a split-coil zero- to 6-Tesla superconducting magnet, with field perpendicular to the gamma ray beam.

Externally applied fields have been used predominantly in material science, physics, and chemistry studies and have only recently become more commonly used to study geologic materials. However, because of the time required and the expense of liquid helium, it still must be considered a non-routine investigation method. In spite of that, Mössbauer experiments using strong external magnetic fields can, in some cases, give important information that is difficult to obtain otherwise (Pankhurst & Pollard, 1990 and 1992). The main applications are in magnetic fluids, magnetic recording, biomagnetism and fundamental research in fine-particle magnetism, where information like interparticle interactions, surface effects and structural and magnetic disorder are important. With fine particle magnetism becoming an important research direction for geologic materials, applied field Mössbauer spectroscopy is becoming a valuable research tool. The Sediment Nanomagnetism group* at the University of Minnesota, (a group of researchers representing several disciplines and in collaboration with several Universities working on synthetic compounds) have begun to utilize the capabilities of the IRM's Mössbauer lab. The group is currently working with nanoparticles of pure and arsenic- and aluminum-doped, ferrihydrite and goethite.

Among the applications cited above, Mössbauer spectroscopy with applied field has been used at IRM by the "Nanogroup" to identify the difference between Néel temperature (T_N) and blocking temperature (T_B). The magnetic hyperfine interaction or nuclear Zeeman effect occurs if the sample is magnetically ordered (when there is a stable magnetic field at the nucleus which can be either intrinsic or from an externally applied field) and splits the spectra into a sextet. With no externally applied field, iron-bearing nanoparticles will have a spectrum consisting of 1 sextet for each phase below its blocking temperature . For nanoparticles, which generally have T_B below 300K, when we increase the temperature from 4.2K the spectrum collapses to a doublet at T_B, which for Mössbauer experiments is when the relaxation time, due to the rapid variations in the lattice magnetization, is less than the Mössbauer transition time of ~ 10^{-8} seconds. Figure 1 reveals the temperature dependence of a nanoferrihydrite. At 4.2K the spectrum shows a magnetically ordered sextet, and as the temperature increases the spectrum collapses to a doublet at ~60K. However, to complicate the matter, the spectrum will also collapse to a doublet above the Néel temperature due to rapid fluctuations of the magnetic field at the nucleus (true paramagnetism), and these two phenomena are indistinguishable with only temperature-dependent ambient-field data. That is, the collapse of a sextet into a doublet on warming cannot be uniquely interpreted as a blocking

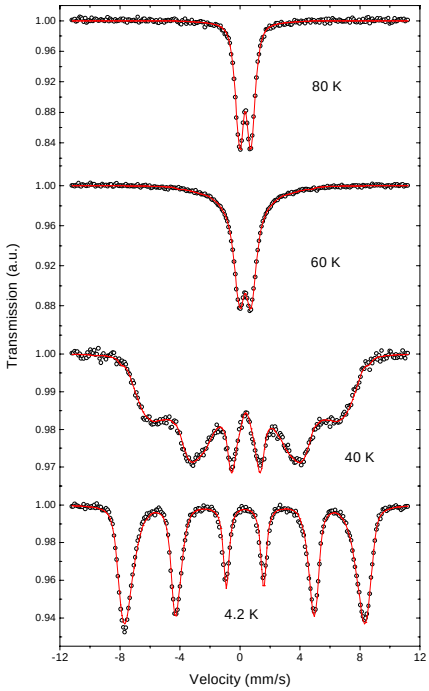

Figure 1 – Evolution of Mössbauer spectra with temperature. The spectra are represented only by a doublet above 60 K, which may or may not represent true T_N (alternatively it may be a nanophase blocking temperature).

*Subir K. Banerjee, R. Lee Penn, Yohan Guyodo, Thelma S. Berquó, Amy Anschutz, Jasmine Erbs, Timothy LaPara and Ramon Egli

continued on p. 11...

Visiting Fellows' Reports

Franziska Brem
ETH-Zürich
brem@mag.ig.erdw.ethz.ch

Magnetic Properties of Human Brain Tissue Related to Epilepsy

Neurodegenerative diseases are thought to be associated with disruption of iron metabolism in the brain; therefore, it is of great interest to know more about the iron phases in the human brain. Low temperature magnetic methods provide a sensitive tool in detecting very small amounts of magnetic phases. The aim of this work is to characterize the magnetic phases in brain tissue from epileptic patients (tumours and hippocampi) and to compare them with properties of non-pathogenic tissue. Three different types of iron phases that have been detected in the human brain are: (1) iron in the blood, heme iron, (2) ferritin, an iron storage protein (10-12 nm in diameter) consisting of a protein shell and a ferrihydrite core, and (3) magnetite, which was first detected in human brain tissue from an autopsy (Kirschvink, *et al.* 1992), and was later found in tissue from epileptic patients (Dobson & Grassi 1996).

The magnetic characteristics of tissue samples are very weak, and thus AC-susceptibility measurements are usually not feasible. To obtain information about the blocking behaviour of ferritin, which is expected to occur below 20 K, the behaviour of DC induced magnetization as a function of temperature is observed in samples cooled in a magnetic field (FC) and in zero-field conditions (ZFC). These measurements were executed on all tissue samples on the MPMS in an applied field of 50 mT. The same set of measurements was carried out on pure blood samples. In the tissue measurements the blood is a background signal to the more interesting tissue signal. By assuming the amount of blood in the tissue, the blood signal can be subtracted. The thermomagnetic curves then show a well-defined average blocking temperature for ferritin at 11 K (Fig.1 left). The bifurcation point of the ZFC and FC curves at about 24 K indicates the start of ordering in the ferritin. For all samples, one or two anomalies are evident in both the ZFC and FC curves between 40 K and 60 K (Fig. 1 right). These unusual features are not artefacts of the equipment, as they have been observed previously in measurements made with another MPMS. Until now, there is no explanation for these anomalies, although they have been observed in pure magnetite single crystals (e.g. Moskowitz, *et al.* 1998). After oxidizing a sample in a humid environment during one week, the anomaly at 54 K disappeared, while the one at 45 K remained. The phase with the higher peak temperature may have been destroyed or it may have changed into the phase with the lower peak temperature. Although magnetite or maghemite with a 10 nm diameter would block around these two temperatures (Liu, *et al*. 2004), we do not believe that the anomalies are due to magnetic blocking since the FC curve tracks the ZFC curve.

One sample showed a stronger DC-signal compared to the others, and AC-susceptibility measurements were tried on it (Fig.2). At low temperature, they verify the results of the induced magnetization measurements. The maxima of the in-phase component at 12 K for 0.1 Hz and 14 K for 1 Hz correspond to the blocking temperatures of the ferritin. In comparison with the AC results, the average blocking temperature at 11 K in the DC induced magnetization measurements is shifted to slightly lower temperatures because the applied field is constant. The quadrature component remains low above 24 K, corresponding to the bifurcation point of the ZFC and FC curves in the induced magnetization measurements. Above this temperature the ferritin becomes fully unblocked.

Thanks to the generous and invaluable support of the IRM-team, I was able to make many measurements that provide valuable information about the magnetic properties of blood and ferritin in human brain tissue. As continuation of the project, new investigations to determine the unknown phases responsible for the signal around 50 K are planned, as well as microscopic work on extracts.

References

Dobson J, Grassi P. 1996 Magnetic properties of human hippocampal tissue - Evaluation of artefact and contamination sources. *Brain Res. Bull.* **39**, 255-259

Kirschvink JL, Kobayashi-Kirschvink A, Diazricci JC, Kirschvink SJ. 1992 Magnetite in Human Tissues - a Mechanism for the Biological Effects of Weak Elf Magnetic-Fields. *Bioelectromagnetics* 101-113

Moskowitz BM, Jackson M, Kissel C. 1998 Low-temperature magnetic behavior of titanomagnetites. *Earth Planet. Sci. Lett.* **157**, 141-149

Liu Q, Jackson M, Yu Y. 2004 Frequency and Temperature Dependence of Superparamagnetism for Magnetite and Maghemite. In press.

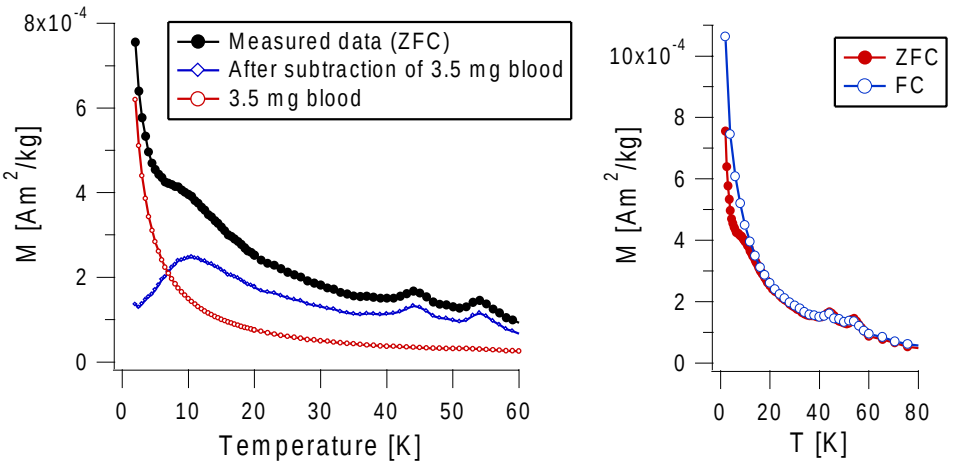

***Fig.1**: ZFC and FC DC-induced magnetization measurements vs temperature in a 50 mT field on a brain tumour tissue and a pure blood sample.*

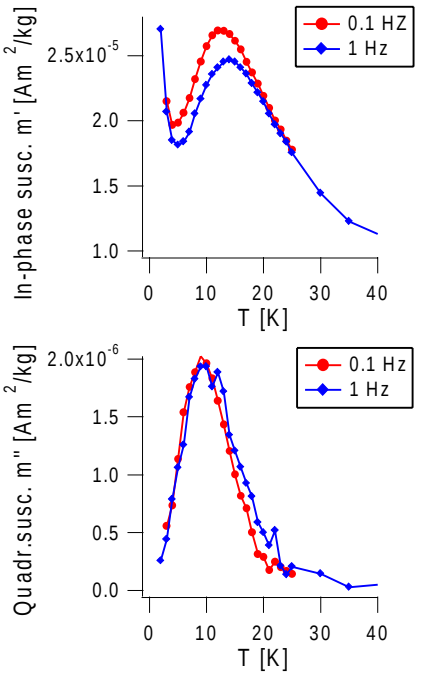

***Fig. 2:** AC- Susceptibility measurements on a tumour tissue*

Adrian Muxworthy
University of Edinburgh
adrian.muxworthy@ed.ac.uk

Understanding Multidomain Remanence: Viscous Magnetization of Multidomain Magnetite

During my visit to the IRM, I made a series of key experiments which are integral to a bigger project currently being undertaken in Edinburgh. This project is examining the viscous behaviour of multidomain (MD) magnetite in attempt to not only understand viscous magnetisation in itself but also to try and unravel remanence acquisition in MD magnetite. We are doing this using a series of complementary techniques; direct measurement of viscous magnetisation and viscous remanent magnetisation acquisition and demagnetisation, and observation of viscous behaviour through the Bitter pattern method as function of time and temperature.

All previous viscous magnetisation measurements we have made have been in relatively low fields of about 0.2 mT. It was of interest to understand the behaviour in higher fields which is possible with the Princeton high-temperature VSM. I examined the possibility of disaccommodation contributing to viscosity by comparing the viscosity of the virgin samples with the viscosity after high-temperature thermal stabilization. The viscosity acquisition constant (the rate of viscosity acquisition) was significantly reduced after thermal stabilization in samples thought to have medium levels of stress (Figure 1). This suggests a disaccommodation contribution to the viscosity in the virgin samples. During viscosity experiments it is normal to measure both viscous acquisition and demagnetisation. Due to the instrument software it was only possible to make acquisition experiments, however, the inability to accurately control the zero field state with the high-temperature VSM meant that this was no great loss

To tie in with the Bitter pattern domain observations, I made some magnetic force microscopy (MFM) images of the same grains to investigate how well the domain structures seen with the Bitter pattern image represent the higher-resolution MFM structures. As expected the MFM revealed much finer detail than that observed by the Bitter pattern image, however, generally the main features were the same, which is encouraging.

I also took the opportunity to measure some Mössbauer spectra on some natural samples involved in another study. Much thanks go to Mike, Thelma and Jim the rest of the IRM'ers for their time, help and patience.

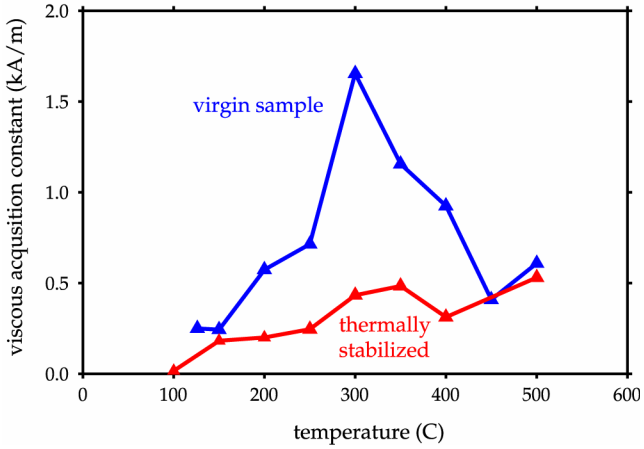

Figure 1. Viscous acquisition constant versus temperature for a commercial synthetic magnetite sample with a mean grain size of ~11 µm. The sample was AF demagnetized at room temperature before each measurement

Jenny Inwood
University of Plymouth
jinwood@plymouth.ac.uk

Rock Magnetic Evidence for a Sea-floor Origin for Magnetic Remanences in a Late Cretaceous Tethyan Ophiolite

The project carried out on my visit to the IRM was to identify and characterize the NRM carriers in rocks from the Hatay Ophiolite of southeastern Turkey. This forms part of my doctoral research which aims to constrain the tectonic history of the Hatay ophiolite, using a combination of palaeomagnetic and structural techniques.

The Hatay ophiolite forms part of a prominent ophiolite chain in the eastern Mediterranean and Middle East which stretches from the Troodos ophiolite of Cyprus eastwards to the Semail ophiolite of Oman. These ophiolites represent fragments of the oceanic lithosphere generated in the Late Cretaceous by supra-subduction zone spreading within a small “Neotethyan” ocean basin. Subsequent closure of Tethys during convergence of the African and Eurasian plates resulted in the emplacement of ophiolitic thrust sheets onto the Arabian continental margin in the Maastrichtian.

The Hatay ophiolite was sampled for palaeomagnetic analysis at various crustal levels, from the cumulate gabbros up to the extrusives, excluding only the serpentinised ultramafics. Specimens from 63 sites were demagnetized in the University of Plymouth laboratory. Demagnetization diagrams show mostly simple rectilinear decay to the origin. Westerly-directed remanences indicate that the ophiolite has experienced large anticlockwise rotations during its history, similar to those previously documented in the coeval Troodos and Baer-Bassit ophiolites. An inclination-only tilt test demonstrates that magnetizations are pre-deformational in origin, despite a complex history of low temperature seafloor alteration, intra-oceanic detachment, thrust emplacement and subsequent neotectonic faulting. Determining precisely what is carrying the stable magnetizations is therefore critical to understanding the magnetic history of the ophiolite.

The magnetic minerals in oceanic crust depend on variables such as the composition and cooling rate of the magma. Research on in situ day oceanic crust has concentrated on the more accessible upper levels, i.e. pillowed and sheet lava flows and sheeted dykes. For a basaltic magma, rapid cooling preserves titanomagnetite with intermediate titanium composition (TM60), whereas slower cooling with deuteric oxidation above the Curie temperature preserves an exsolution texture of near-ilmenite and near-magnetite lamellae (O’Reilly, 1984). Low temperature oxidation at ambient temperatures on the seafloor oxidises (titano)magnetite to (titano)maghemetite due to leaching of the iron by seawater. This can alter to magnetite during subsequent low-temperature inversion (O’Reilly, 1984). The magnetic minerals carrying the pre-deformational remanence in the ophiolite were anticipated to be either those observed within in situ oceanic crust, or an inversion that allows an early magnetization to be retained, with potential variations between the different lithologies sampled.

Preliminary Rock Magnetic Results from the University of Plymouth

1. Analyses of IRM acquisition for at least one sample per site indicated a dominance of low coercivities for all samples.

VF Reports

continued on p. 4...

continued from p. 3

2. Stepwise thermal demagnetization of natural remanences indicated differences in unblocking temperatures (T_B) between lithologies. The deeper levels (gabbros and cumulate gabbros) had T_Bs near 580°C suggesting the presence of Ti-poor magnetite. For the pillow lavas T_Bs were generally lower, suggesting a higher titanium content. More variable T_Bs were observed for the sheeted dyke complex with a maximum T_B of 560-580°C, but also in some samples a lower temperature component was observed to unblock at 350-400°C.
3. Alternating field demagnetization characteristics were consistent with the presence of both MD to SSD grains with median destructive fields ranging from 5 mT to >40 mT.

EXPERIMENTS PERFORMED AT THE IRM

1. Hysteresis loops were determined for 135 cores using the Princeton Applied Research VSM, with coercivity of remanence (Hcr) also measured.
2. Curie point (T_C) determinations were carried out using the Princeton Measurements MicroMag VSM on 51 powdered samples.
3. Low temperature experiments using the Quantum Design Magnetic Property Measurement System (MPMS) were carried out on 54 powdered samples. Thermomagnetic curves were obtained by cooling a room temperature (RT) SIRM acquired in a 2.5 T field from 300 to 10K, and by imparting a low temperature (LT) SIRM in a 2.5 T field and warming the sample from 10 to 300K. For selected samples, both cooling and warming curves of RT SIRM were plotted, as was the curve following cooling of the sample both in field (FC) and in zero field (ZFC).
4. Alternating current (AC) susceptibility measurements as a function of frequency were taken for eight samples using the MPMS and the Lakeshore AC Susceptometer.

RESULTS

The majority of samples of all lithologies lie within the PSD field of a Day plot (Figure 1). The sheeted dyke complex showed more variation with some samples falling in the MD field.

Deeper levels of the ophiolite had Curie points near that of Ti-poor magnetite with a mean T_C value close to 590°C in both the gabbros and sheeted dyke complex. Heating and cooling curves were reversible in the majority of samples. The pillow lavas had T_Cs ranging from 475 to 560°C with a mean of 530°C. These lower temperatures suggest the presence of a higher titanium phase than for the gabbros, although these Tcs are higher than that of TM60. Two components were observed in some samples at temperatures between 335 and 400°C, with all except two of these samples being from the sheeted dyke complex.

Low temperature runs allow easy recognition of the Verwey transition in magnetite on both the warming and cooling curves if it is present. The

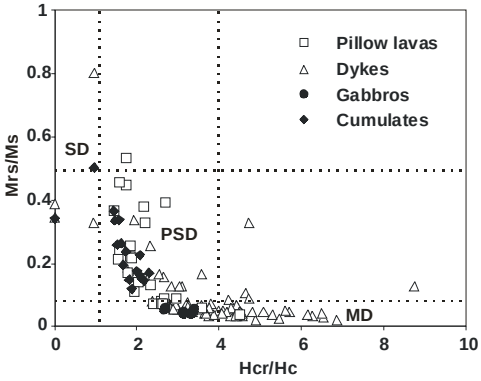

Figure 1: A Day plot of the 135 samples measured on the VSM.

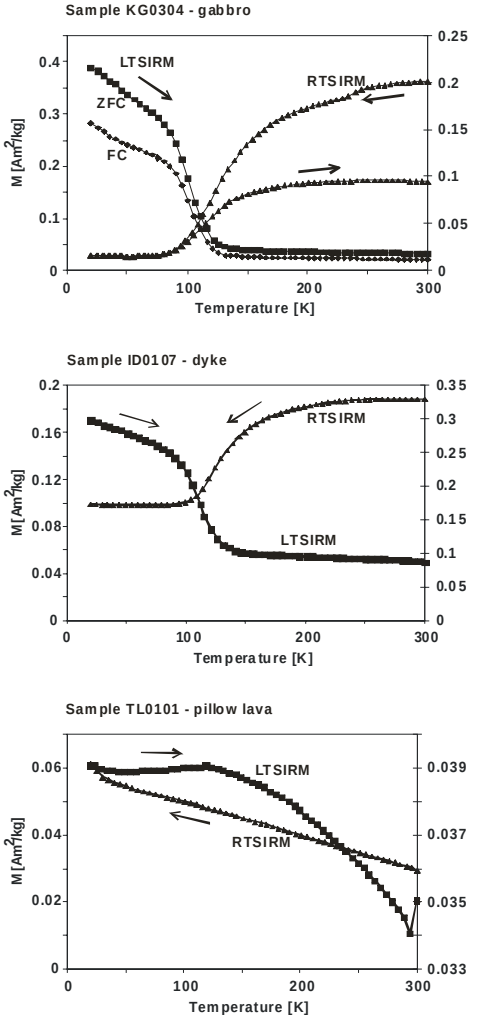

Figure 2: Low temperature thermomagnetic curves of saturation remanence for a representative sample from each main lithology: (i) gabbro sample, clearly showing the Verwey transition; (ii) sample from the sheeted dyke complex showing the Verwey transition; (iii) basaltic lava sample showing a 'smeared out' curve suggesting presence of a higher degree of titanium than in the other samples.

transition occurs at 120K in stoichiometric magnetite, but is decreased by oxidation or the presence of impurities such as titanium (Muxworthy and McClelland, 2000). The dykes and lower crustal lithologies all displayed clear low temperature transitions in the vicinity of 110K. In some of the cumulate gabbros the step was 'smeared' out, probably due to the presence of more oxidised magnetite (Figure 2(i), 2(ii)) (Özdemir et al. 1993, 2002). In the pillow lavas, the Verwey transition was generally not clear, and a considerably more gradual change in magnetization was seen on the warming curve (Figure 2(iii)). This, combined with the lower Curie temperatures, implies that a higher degree of titanium substitution in the pillow lavas minimises the effect of the Verwey transition.

SUMMARY

The results obtained at the IRM are compatible with the presence of fine magnetic grain sizes capable of retaining a stable magnetization throughout the complex history of the ophiolite, with PSD grains dominant in the majority of samples. There is a difference in magnetic mineralogy depending on the crustal level. The clear Verwey transitions and high T_Cs of the deeper levels of the crust indicate that Ti-poor titanomagnetite/magnetite is the major carrier of the magnetic signal, and the absence of the Verwey transition and lower T_Cs of the higher crustal levels indicate the presence of a more Ti-rich titanomagnetite. These mineralogies are compatible with acquisition of stable remanences on the seafloor soon after genesis of the ophiolitic crust at an oceanic spreading centre.

Complementary Analyses

In order to support the rock magnetic results obtained at the IRM, I have used a JSM6100 SEM with an Oxford INCA x-ray microanalyser at the University of Plymouth to study representative samples. This confirms the presence in the gabbros of near-magnetite and near-ilmenite in very well-developed exsolution lamellae in large grains (up to 1mm). The pillow lavas were observed to contain grains with higher levels of titanium, as concluded from the rock magnetic results. The dykes contained a mixture of near magnetite grains, more titanium rich grains, as well as the presence of some grains displaying exsolution. Skeletal and cubic crystals were common, supporting the existence of a primary remanence.

I would like to thank everyone I met at the IRM for being so helpful, for showing me how to use the instruments and for helping with the interpretation of results.

REFERENCES

Muxworthy, A.R. and E. McClelland, 2000. Review of the low-temperature magnetic properties of magnetite from a rock magnetic perspective. *Geophys. J. Int., 104:* 101-114.

O'Reilly, W., 1984. *Rock and mineral magnetism*. Blackie.

Özdemir, Ö., D. J Dunlop and B. M. Moskowitz, 1993. The effect of oxidation on the Verwey transition in magnetite. *Geophys. Res. Letters., 20*: 1671-1674.

Özdemir, Ö., D.J. Dunlop and B.M. Moskowitz, 2002. Changes in remanence, coercivity and domain state at low temperature in magnetite, *Earth and Planetary Science Letters, 194*: 343-358.

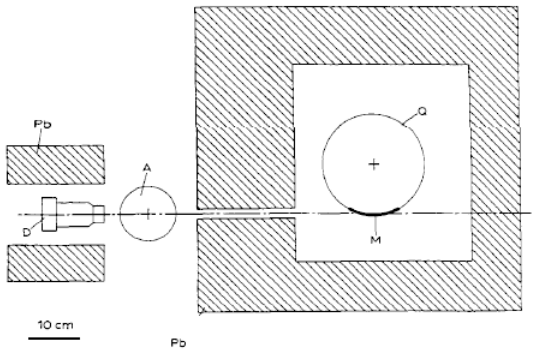

Fig. 7. Experimental arrangement. A, absorber-cryostat; Q, rotating cryostat with source; D, scintillation detector.

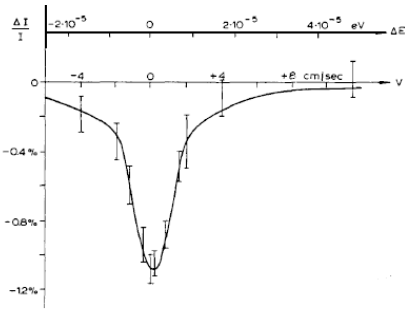

Fig. 8. Relative intensity ratio $\Delta I/I$ of gamma radiation measured behind the resonant iridium absorber, in comparison with intensities measured behind a nonresonant absorber.

The first Mössbauer spectrum, measured in 1958 for ^{191}Ir using an ^{191}Os source. "Since the conical-gear assembly necessary for adjusting the various velocities caused a disagreeable delay in this experiment which was so exciting for me, I took advantage of the existence in Germany of a highly developed industry for the production of mechanical toys. A day spent in the Heidelberg toy shops contributed materially to the acceleration of the work." *Mössbauer, R. L., Recoilless nuclear resonance absorption of gamma radiation, Nobel Lecture, December 11, 1961.* Published in: *Nobel Lectures. Physics 1942-1962*, Elsevier Publishing Company, Amsterdam, 1964.

Current Abstracts

A list of current research articles dealing with various topics in the physics and chemistry of magnetism is a regular feature of the IRM Quarterly. *Articles published in familiar geology and geophysics journals are included; special emphasis is given to current articles from physics, chemistry, and materials-science journals. Most abstracts are culled from* INSPEC *(© Institution of Electrical Engineers),* Geophysical Abstracts in Press *(© American Geophysical Union), and* The Earth and Planetary Express *(© Elsevier Science Publishers, B.V.), after which they are subjected to Procrustean editing and condensation for this newsletter. An extensive reference list of articles (primarily about rock magnetism, the physics and chemistry of magnetism, and some paleomagnetism) is continually updated at the* IRM. *This list, with more than 5200 references, is available free of charge. Your contributions both to the list and to the Abstracts section of the* IRM Quarterly *are always welcome.*

Alteration & Remagnetization

Blumstein, A. M., *et al.*, 2004, **Paleomagnetic dating of burial diagenesis in Mississippian carbonates, Utah**: *J. Geophys. Res., v.109,* no.B4, doi:10.1029/2003JB002698.
Paleomagnetic and rock magnetic results show two ancient secondary magnetizations residing in magnetite, interpreted to be chemical remanent magnetizations (CRMs). Modeling of the smectite-to-illite transformation suggests a mean age prior to acquisition of both CRMs, although the range for illitization overlaps with the Triassic to Jurassic CRM. The results of this study support the hypothesis that pervasive CRMs can be related to burial diagenetic processes.

Geissman, J. W. and Harlan, S. S., 2004, **Paleomagnetic and rock magnetic evidence for a secondary yet early magnetization in large sandstone pipes and host Late Middle Jurassic (Callovian) Summerville Formation and Bluff Sandstone near Mesita, west central New Mexico**: *Journal of Geophysical Research-Solid Earth, v.109,* no.B7, doi:10.1029/2003JB002463.
The similarity in demagnetization properties between pipes and adjacent host strata, the absence of a well-defined high-T_{UB} remanence, and the essentially uniform reverse polarity indicate that pipes and host strata contain secondary magnetizations acquired during and after pipe injection. We propose that acquisition of the secondary magnetization took place in the presence of alkaline, high pH brines formed by the dissolution of the underlying gypsum-dominated strata.

Liu, J., *et al.*, 2004, **High-resolution analysis of early diagenetic effects on magnetic minerals in post-middle-Holocene continental shelf sediments from the Korea Strait**: *J. Geophys. Res., v.109,* no.B3, doi:10.1029/2003JB002813.
These rapidly deposited sediments contain four intervals of contrasting chemical and magnetic properties: 1 (shallowest) - highest concentrations of detrital magnetite and hematite, and the lowest solid-phase sulfur contents; 2 - pyrite and sharply decreasing magnetite and hematite concentrations; 3 - progressive loss of hematite with depth, and minimum magnetite concentration; 4 - an increasing down-core enhancement of authigenic greigite, formed due to arrested pyritization reactions.

Otofuji, Y., *et al.*, 2003, **Cenozoic remagnetization of the Paleozoic rocks in the Kitakami massif of northeast Japan, and its tectonic implications**: *Earth and Planetary Science Letters, v.210,* p. 203-17.
These rocks were remagnetized between 62 and 16 Ma. The secondary magnetization of the serpentinized ultramafic rocks is carried by magnetite, which grew in veins and mesh rims of serpentine, whereas the carrier of the magnetization in limestones is fine-grained pyrrhotite. Since serpentinization requires fluid migration, one of the most likely events is the eastward lateral migration of water into the Kitakami massif, which we attribute to Cenozoic suturing of the Kitakami massif with the Asian continent.

Anisotropy

Cifelli, F., Mattei, M., Hirt, A. M. and Günther, A., 2004, **The origin of tectonic fabrics in "undeformed" clays: The early stages of deformation in extensional sedimentary basins**: *Geophys. Res. Lett., v.31,* no.9, doi:10.1029/2004GL019609.
Low- and high-field AMS and mineral fabric deduced by neutron texture analysis show penetrative deformation on a grain-scale. The well-defined tectonic magnetic lineation is parallel to the stretching direction and located at the intersection of the basal planes of phyllosilicates, forming grain-scale folds and crenulations. This spatial configuration reflects basin scale deformation processes and suggests the existence of a nearly uniaxial stress field during the incipient extensional phases.

Hansen, A., *et al.*, 2004, **Neutron pole figures compared with magnetic preferred orientations of different rock types**: *Physica B: Condensed Matter, v.350,* no.1-3, p.120-122.
Neutron diffraction is an excellent tool for pole figure measurement of rock samples. Due to high penetration depth for most materials neutron diffraction represents an efficient tool to measure complete pole figures with reliable grain statistics even in coarse grained or inequi-granular materials. Here we compare neutron pole figures with AMS results for various deformed rocks.

Krijgsman, W. and Tauxe, L., 2004, **Shallow bias in Mediterranean paleomagnetic directions caused by inclination error**: *Earth and Planetary Science Letters, v.222,* no.2, p.685-695.
In addition to the well-known variation of magnetic inclination with latitude, the N-S elongation of directional dispersion also varies. For Miocene sediments from Spain and Crete we invert the inclinations using a range of "flattening factors" to find the elongation/inclination pair consistent with a statistical model for the paleosecular variation. We conclude that the east Mediterranean inclination anomaly is caused by sedimentary inclination error and not by a persistent octupolar contribution to the geomagnetic field, or northward transport.

Poland, M. P., Fink, J. H. and Tauxe, L., 2004, **Patterns of magma flow in segmented silicic dikes at Summer Coon volcano, Colorado: AMS and thin section analysis**: *Earth and Planetary Science Letters, v.219,* no.1-2, p.155-169.
Two intrusions are broken into multiple segments that suggest vertical dike propagation, but AMS measurements and thin section observations suggest that magma flow was often subhorizontal and away from the center of the volcano. Segments that are proximal to the central intrusion are characterized by magma that flowed steeply upward at the proximal segment extremity, then laterally along the segment, and finally downward at the distal end of the segment. Magma flow in offset segment tips located far from the volcano center was subhorizontal towards the adjacent segment, implying lateral propagation of segment tips towards one another.

Data Processing and Analysis

Borradaile, G. J. and Hamilton, T., 2003, **Limestones distinguished by magnetic hysteresis in three-dimensional projections**: *Geophysical Research Letters, v.30*, no.18, doi:10.1029/2003GL017892.
Limestone samples are simply discriminated in a new 2D projection produced by projecting hysteresis data from three dimensions (z, y, x=M_r/M_s, B_{cr}, B_c) onto a plane containing the M_r/M_s axis. The orientation of the plane is controlled by its x´-axis that is defined by a suitably selected B_{cr}/B_c ratio, most often in the magnetite PSD range, $2<(B_{cr}/B_c)<4$.

Fabian, K., 2003, **Some additional parameters to estimate domain state from isothermal magnetization measurements**: *Earth and Planetary Science Letters, v.213*, p. 337-45.
For the quantitative analysis of domain state, four parameters are proposed and their theoretical background is discussed. Two of them, a hysteresis shape parameter and a coercivity ratio, can be directly calculated from standard measurements of the hysteresis loop and backfield curve. The other two, a transient energy dissipation ratio and the viscosity of isothermal remanent magnetization, require additional measurements, which, however, do not increase measurement time noticeably. Their utility is shown for a set of synthetic magnetite and titanomagnetite samples and in a transect from the rim to the center of a dredged mid-ocean ridge basalt.

Environmental Magnetism and Paleoclimate Proxies

Chaparro, M. A. E., *et al.*, 2004, **Relevant magnetic parameters and heavy metals from relatively polluted stream sediments - Vertical and longitudinal distribution along a cross-city stream in Buenos Aires Province, Argentina**: *Studia Geophysica et Geodaetica, v.48*, no.3, p.615-636.
Positive correlations were obtained between magnetic parameters (κ, ARM, S-ratio and κ_{ARM}/κ) and contents of heavy metals, with more significant correlations for mineral- and grainsize-dependent parameters (κ_{ARM}/κ and S-ratio) than for magnetic concentration-dependent parameters. Therefore, the κ_{ARM}/κ and the S-ratio seem to be the most relevant magnetic parameters to describe the vertical and longitudinal distribution of heavy metals present in these stream sediments.

Deng, C., *et al.*, 2004, **Mineral magnetic properties of loess/paleosol couplets of the central loess plateau of China over the last 1.2 Myr**: *J. Geophys. Res., v.109*, no.B1, doi:10.1029/2003JB002532.
In 15 loess-paleosol couplets (S0/L1 to S14/L15) from the Jiaodao section, magnetic parameters display systematic variations related to paleoclimate variations and intensity of pedogenesis. High-temperature susceptibility curves of paleosols show a generally decreasing trend in reversibility from the base of the Lishi Formation to the Holocene black loam, possibly indicating a decrease in weathering intensity.

Jovane, L., Florindo, F. and Dinarès-Turell, J. , 2004, **Environmental magnetic record of paleoclimate change from the Eocene-Oligocene stratotype section, Massignano, Italy**: *Geophysical Research Letters, v.* 31, L15601, doi:10.1029/2004GL020554.
A high-resolution environmental magnetic study reveals alternating intervals with high and low magnetic mineral concentrations similar to the pattern of rock magnetic property variations observed from an environmental magnetic study of the CIROS-1 sediment core from Antarctica. These results suggest that an external forcing mechanism drove the sedimentary response to global climate change prior to the major Oi-1 cooling event at the Eocene-Oligocene boundary.

Liu, Q.S., *et al.*, 2004, **Grain sizes of susceptibility and anhysteretic remanent magnetization carriers in Chinese loess/paleosol sequences**: *J. Geophys. Res., v.109*, no.B3, doi:10.1029/2003JB002747.
Detailed studies show that χ and ARM of the Chinese loess/paleosol sequences are carried by almost identical magnetic carriers. Therefore the ratio $(\chi - \chi_0)/\chi_{ARM}$ (where χ_0 is the intercept susceptibility of the plot of χ versus ARM) can be used to quantify their grain size. By determining this ratio for three Chinese loess/paleosol profiles with different degrees of pedogenesis and sedimentation rates, we show that the lower grain-size limit of aeolian magnetic particles in the loess units is about 100–300 nm (fine PSD). In contrast, pedogenically produced magnetic particles for mature paleosols dominantly cover both the SP and SD ranges.

Extraterrestrial Magnetism

Antretter, M., *et al.*, 2003, **Paleomagnetic record of Martian meteorite ALH84001**: *Journal of Geophysical Research, v.108*, no.E6, doi:10.1029/2002JE001979, 2003.
The NRM of ALH84001 is predominantly carried by fine magnetite, which is in epitaxial and topotactic relation with carbonate, from which it formed in the major impact event at 4.0 Ga. Normalizing NRM intensity by SIRM gives an estimate for the 4.0 Ga Martian field one order smaller than the present geomagnetic field, unlikely to be strong enough to generate the high-intensity Martian magnetic anomalies. ALH 84001 in its pristine state as an orthopyroxenite is not a plausible source rock for the Martian anomalies because its magnetite was not formed until the 4.0 Ga event.

Magnetic Field Records and Paleointensity Methods

Biggin, A. J. and Thomas, D. N., 2003, **The application of acceptance criteria to results of Thellier palaeointensity experiments performed on samples with pseudo-single-domain-like characteristics**: *Physics of the Earth and Planetary Interiors, v.138*, p.3-4.
The results of a simulated Thellier palaeointensity experiment show that: pTRM checks can fail despite no alteration occurring, pTRM tail checks are not reliable as indicators of MD-like behaviour, room temperature susceptibility monitoring is unreliable for detecting alteration, and that the minimum requirement for the f (fraction)-value should be increased from 0.15 to at least 0.5.

Bohnel, H., *et al.*, 2003, **Microwave palaeointensities from a recent Mexican lava flow, baked sediments and reheated pottery**: *Earth and Planetary Science Letters, v.214*, p. 221-36.
Microwave PI determinations for a 1670-yr old lava flow produced high-quality estimates with a mean of 58.3±9.5 μT; previous Thellier-Coe measurements were of much lower quality, producing a higher mean of 67.9±9.8 μT (25 out of 65 samples). Pottery fragments recovered from the contact zone between the lava flow and the underlying baked sediments seem to be less suitable for PI determinations, because they contain larger magnetic grains and are more prone to thermally induced alteration than the lava samples.

Carvallo, C., *et al.*, 2003, **Mono Lake or Laschamp geomagnetic event recorded from lava flows in Amsterdam Island (southeastern Indian Ocean)**: *Geophysical Journal International, v.154*, no.3, p.767-82.
In four basalt flows, normal polarity is found for two units and an intermediate direction for the other two. Half of the samples yielded reliable paleointensity values: the normal units yield VDMs of 6.2 and 7.7 (10^{22} A m^2) and the excursional units yield 3.7 and 3.4 (10^{22} A m^2). $^{40}Ar/^{39}Ar$ isotopic age determinations provide an estimate of 26±15 and 18±9 kyr for the transitional lava flows, which could correspond to the Mono Lake excursion. However, the large error bars do not exclude the hypothesis that this event is the Laschamp.

Dunlop, D. J. and Yu, Y., 2003, **Testing an inverse Thellier method of paleointensity determination**: *Journal of Geophysical Research, v.108*, no.B9, doi:10.1029/2003JB002469.
Instead of heating-cooling steps, a new inverse Thellier method uses cooling-heating steps below room temperature T_0 to determine paleointensity from inverse TRM (ITRM, produced when magnetite warms from below T_V to T_0 in a field H), or from other types of NRM that have LTD spectra resembling that of ITRM. In our experiments, NRM was an ITRM, and we measured magnetites with mean grain sizes from 0.065 to 135 μm and two gabbros containing elongated SD magnetite. SD samples had quasilinear inverse Arai plots but other samples had convex-down curves, with more ITRM lost in zero-field steps than is regained as pITRM during in-field steps. However, the inverse Thellier method may have more linear behavior if the NRM is a TRM because the greater resistance of TRM to LTD should offset the too-rapid decay of ITRM in zero-field steps.

Frank, U., Schwab, M. J. and Negendank, J. F. W., 2003, **Results of rock magnetic investigations and relative paleointensity determinations on lacustrine sediments from Birkat Ram, Golan Heights (Israel)**: *Journal of Geophysical Research, v.108*, no.B8, doi:10.1029/2002JB002049.

This profile is supposed to span the Late Holocene. Titanomagnetites in the PSD range are the main magnetic carriers in the homogenous sediments. The relative paleointensity was estimated by normalizing $J_{NRM(20\ mT)}$ by different concentration parameters. The median destructive field of the NRM (MDF_{NRM}) is coherent with the relative paleointensity estimates, indicating that a sedimentary effect has not sufficiently been removed by the normalization process. Therefore a second normalization, based on the linear relationship between the paleointensity estimates and the MDF_{NRM}, was applied, resulting in an improvement of the records.

Geiss, C. E. and Banerjee, S. K., 2003, **A Holocene-late Pleistocene geomagnetic inclination record from Grandfather Lake, SW Alaska**: *Geophysical Journal International, v.153,* no.2, p.497-507.
The first inclination record for Alaska that spans the entire Holocene is well dated by seven AMS radiocarbon dates. Its magnetic component consists of PSD (5-15 μm) magnetite that occurs in concentrations ranging from 10 to 1000 ppm. Some samples may also contain titanomagnetite (TM30) as a minor component. The record shows several features between present and 15 ka BP, which shed light on the short-term behaviour of the geomagnetic field at high latitudes and can be used for site correlations.

Goguitchaichvili, A., *et al.*, 2004, **Absolute geomagnetic paleointensity after the Cretaceous Normal Superchron and just prior to the Cretaceous-Tertiary transition**: *J. Geophys. Res., v.109,* no.B1, doi:10.1029/2003JB002477.
Thirty-nine samples from eight cooling units were selected for paleointensity experiments on the basis of their low-viscosity index, stable remanent magnetization, and close to reversible continuous thermomagnetic curves. High-quality determinations were obtained for 18 individual samples from four independent lava flows, yielding a VDM of is $4.9 \pm 0.6 \times 10^{22}$ A m^2. A careful examination of high-quality paleointensity data from Cretaceous shows no simple relation between field strength and reversal rate.

Goguitchaichvili, A., *et al.*, 2004, **Pre-Columbian mural paintings from Mesoamerica as geomagnetic field recorders**: *Geophys. Res. Lett., v.31,* no.12, doi:10.1029/2004GL020065.
A reconnaissance archeomagnetic study shows that at least four murals retain a remanent magnetization carried by a mixture of magnetite and minor hematite grains. In most specimens, a ChRM is successfully isolated by AF demagnetization, with mean directions within the range of secular variation during the last centuries. The archeomagnetic study of pre-Columbian mural paintings opens new alternatives to drawing a reliable reference master curve for the region.

Horng, C.-S., Roberts, A. P. and Liang, W.-T., 2003, **A 2.14-Myr astronomically tuned record of relative geomagnetic paleointensity from the western Philippine Sea**: *Journal of Geophysical Research, v.108,* no.B1, doi:10.1029/2001JB001698.
PSD titanomagnetite is the only magnetic mineral identified and variations in concentration fall well within the accepted limits for relative PI variations. No significant temporally persistent periodicities are observed in wavelet analyses of the PI time series or in the rock magnetic parameters used for RPI normalization. The record is highly coherent with the Sint-800 stack and with a coeval record from the West Caroline Basin. We observe neither an asymmetrical sawtooth form nor any persistent orbital periodicity.

Jordanova, N., Kovacheva, M., Hedley, I. and Kostadinova, M., 2003, **On the suitability of baked clay for archaeomagnetic studies as deduced from detailed rock-magnetic studies**: *Geophysical Journal International, v.153,* no.1, p.146-58.
The most important factors influencing the magnetic behaviour are the degree of heating in antiquity, the initial composition of the unbaked material and the burial conditions. The large difference in heating temperatures within a particular archaeological feature is a major cause of variation in magnetic behaviour amongst individual specimens. Nevertheless, the study has shown a very good coincidence between rock-magnetic characteristics and the success rate in palaeointensity evaluation.

Kostadinova, M., Jordanova, N., Jordanova, D. and Kovacheva, M., 2004, **Preliminary study on the effect of water glass impregnation on the rock-magnetic properties of baked clay**: *Studia Geophysica et Geodaetica, v.48,* no.3, p.637-646.
A common practice in archaeomagnetic studies in many laboratories is the impregnation of the material with water glass (siliceous gel) in order to achieve better consolidation before cutting. Experiments designed to monitor the alterations in isothermal remanence and magnetic susceptibility for two sets of specimens-non-impregnated and impregnated with water glass show that water glass can cause considerable changes in magnetic susceptibility, but the remanent magnetization is not influenced significantly.

Morales, J., Goguitchaichvili, A. and Urrutia-Fucugauchi, J., 2003, **An experimental evaluation of Shaw's paleointensity method and its modifications using Late Quaternary basalts**: *Physics of the Earth and Planetary Interiors, v.138,* no.1, p.1-10.
Absolute paleointensity experiments were carried out using Shaw's method and its modifications on 49 samples selected because of their low viscosity index, stable remanent magnetization, nearly reversible thermomagnetic curves, and high quality Thellier paleointensity results. Only 13 samples yielded acceptable results using Shaw's original method, only one using Rolph and Shaw's method, and none using Kono's modification. The extremely low success rates may be due to magneto-chemical changes during heating.

Plenier, G., Camps, P., Coe, R. S. and Perrin, M., 2003, **Absolute palaeointensity of Oligocene (28-30 Ma) lava flows from the Kerguelen Archipelago (southern Indian Ocean)**: *Geophysical Journal International, v.154,* no.3, p.877-90.
VDMs calculated for these flows vary from 2.78 to $9.47*10^{22}$ A m^2 with an arithmetic mean value of $6.15\pm2.1*10^{22}$ A m^2, resulting in a higher ($5.4\pm2.3*10^{22}$ A m^2) Oligocene mean VDM than previously reported, identical to the $5.5\pm2.4*10^{22}$ A m^2 mean VDM obtained for the 0.3-5 Ma time window. The new estimates strengthen the conclusion that the recent geomagnetic field strength is anomalously high compared to that older than 0.3 Ma.

Tauxe, L. and Staudigel, H., 2004, **Strength of the geomagnetic field in the Cretaceous Normal Superchron: New data from submarine basaltic glass of the Troodos Ophiolite**: *Geochemistry Geophysics Geosystems, v.5,* doi:10.1029/2003GC000635.
New paleointensity data suggest a dipole strength (81 ± 43 ZAm^2; Z = 10^{21}) equivalent to the present field or nearly twice the post-CNS average. These results agree remarkably well with those predicted from the long paleointensity record derived from DSDP Site 522. The new data set for the CNS suggests a strong and stable field during the period when it stopped reversing. Moreover, the similarity of the CNS data with the present geomagnetic field suggests that it is presently in a state of unusual polarity stability.

Walton, D., 2004, **Avoiding mineral alteration during microwave magnetization**: *Geophys. Res. Lett., v.31,* no.3, doi:10.1029/2003GL019011.
Recent microwave results reveal evidence of mineral alteration. This letter examines the energy absorption by the magnetic nanoparticles, and the heat flow to the matrix. It is shown that, since the temperature difference between the magnetic grains and the matrix is proportional to the power density at the sample, increasing the power density sufficiently can limit the matrix temperature increase to a few degrees, completely eliminating any possibility of mineral alteration.

Xu, S. and Dunlop, D. J., 2004, **Thellier paleointensity theory and experiments for multidomain grains**: *J. Geophys. Res., v.109,* no.B7, doi:10.1029/2004JB003024.
Extended theories of TRM and pTRM in MD grains, modeling steps in Thellier paleointensity determination, agree semiquantitatively with experimental results for parallel and perpendicular pTRMs for large MD magnetites (135 μm). Straight line fits through low- and medium-T points in Arai plots of MD (135 μm) grains overestimated the paleofield by as much as 100%; and for small PSD (0.6 and 1 μm) grains overestimated by about 25%. However, by using linear segments of medium- to high-T data with f values >0.5 it may be possible to obtain reasonable paleointensity estimates even for larger PSD (6 and 20 μm) and MD grains. Middle- to high-T fits for 0.6 μm grains gave paleointensities within 4% of the correct value, utilizing essentially the entire data set (f > 0.9). Perpendicular data always gave superior linear fits. Orienting samples with their NRMs perpendicular to the laboratory field is therefore recommended for rocks containing PSD and MD grains. However,

double heatings are preferable to single heatings because they allow pTRM tail checks to be carried out.

Yamamoto, Y., Tsunakawa, H. and Shibuya, H., 2003, **Palaeointensity study of the Hawaiian 1960 lava: implications for possible causes of erroneously high intensities**: *Geophysical Journal International, v.153*, no.1, p.263-76.
For 19 cores classified into three groups with degrees of the deuteric oxidation, Coe's version of the Thellier method yielded a mean of 49.0±9.6 μT (N=17), higher than the IGRF (36.2 μT). A dependence on the oxidation indices can be explained by TCRM acquisition during the cooling of the lava. The double-heating technique (DHT) of the Shaw method combined with LTD (LTD-DHT Shaw method) gave a better average of 39.4±7.9 μT (N=9), though the success rate was much lower. The results of both methods emphasize the importance of taking and measuring samples from the parts of various oxidation degrees in a lava flow.

Yoshihara, A., Kondo, A., Ohno, M. and Hamano, Y., 2003, **Secular variation of the geomagnetic field intensity during the past 2000 years in Japan**: *Earth and Planetary Science Letters, v.210*, p. 219-31.
Thellier paleointensity determinations for 10 eruptive units of Izu-Oshima and Fuji show good consistency with previous archaeointensity and paleointensity results, allowing us to construct a reference curve of the field intensity variation for the past 2000 yr in Japan. The reference curve has a general trend of decreasing intensity since AD 500, showing two peaks of the field strength around AD 500 and 1400 and two troughs around AD 1200 and 1700.

Yu, Y. J., Tauxe, L. and Genevey, A., 2004, **Toward an optimal geomagnetic field intensity determination technique**: *Geochemistry Geophysics Geosystems, v.5*, doi:10.1029/2003GC000630.
A simple mathematical model shows that both the zero-field first (ZI) and infield first (IZ) methods have a strong angular dependence on the laboratory field H_{lab} (parallel, orthogonal, and antiparallel) while the two in-field steps method is independent of the direction of the laboratory-produced field. The ZI method with H_{lab} anti-parallel to the NRM is the most robust paleointensity determination technique when $H_{lab}<H_{paleo}$. However, the ZI method with H_{lab} parallel to the NRM is the optimum approach when $H_{lab}>H_{paleo}$. By far the best approach, however, is to alternate the IZ steps with ZI steps.

Magnetic Microscopy and Spectroscopy

Berdunov, N., Murphy, S., Mariotto, G. and Shvets, I. V., 2004, **Atomically resolved spin-dependent tunneling on the oxygen-terminated Fe_3O_4(111)**: *Physical Review Letters, v.93*, no.5, 057201.
We employ spin-polarized STM to study the spin-dependent tunneling between a magnetite (111) sample and an antiferromagnetic tip through a vacuum barrier at room temperature. Atomic scale STM images show significant magnetic contrast corresponding to variations in the local surface states induced by oxygen vacancies. The estimated variations in tunneling magnetoresistance of 250% suggest that the spin-transport properties are significantly altered locally by the presence of surface defects.

Fauth, K., Goering, E., Schutz, G. and Kuhn, L. T., 2004, **Probing composition and interfacial interaction in oxide passivated core-shell iron nanoparticles by combining x-ray absorption and magnetic circular dichroism**: *Journal of Applied Physics, v.96*, no.1, p.399-403.
We present x-ray absorption and x-ray magnetic circular dichroism studies of iron oxide passivated iron nanoparticles. The combination of measurements with different probing depths allows us to determine the oxide composition while the magnetic data reveal the magnetic interactions across the interface between the α-Fe core and the spin canted ferrimagnetic iron oxide shell. These studies shed light on the mechanisms that govern the magnetic properties of core-shell nanoparticles.

Kim-Ngan, N. T. H., Soszka, W., Jaglo, G. and Goc-Jaglo, D., 2004, **Surface metal-insulator phase transition of a single crystalline magnetite (001)**: *Journal of Magnetism and Magnetic Materials, v.268*, p. 49-56.
The single crystalline Fe_3O_4 (001) surface has been investigated by using a low-energy ion scattering (LEIS) in the temperature range of 85-300 K. In the metal-insulator phase transition region, the temperature-dependence of the scattering ion yield, $R^+(T)$ shows two step-like increases, the first always at 138 K, and the second at 123 K under 5 keV Ar ion bombardment, and moving to lower temperature with increasing primary energies.

Magnetization & Demagnetization Processes

Dunlop, D. J., Xu, S. and Heider, F., 2004, **Alternating field demagnetization, single-domain-like memory, and the Lowrie-Fuller test of multidomain magnetite grains (0.6–356 μm)**: *J. Geophys. Res., v.109*, no.B7, doi:10.1029/2004JB003006.
For two sets of sized crushed magnetites (0.6, 1, 3, 6, 9, 14, 20, 110, and 135 μm), one set unannealed and the other annealed, and a set of hydrothermally grown magnetites (0.8, 6.3, 25, 64, 94, and 356 μm), TRM and SIRM memories after LTD are much harder to AF demagnetize than the original remanences. In high-stress unannealed grains, after-LTD response depends on grain size, larger grains demagnetizing more easily than smaller ones. In low-stress annealed and hydrothermal magnetites, after-LTD response is almost independent of grain size over nearly 3 decades. We propose an ad hoc model in which LTD triggers domain wall unpinning and nucleation events up to a coercivity threshold, producing the observed initial plateaus in AF demagnetization curves of TRM and SIRM memories. The size-independent demagnetization behavior of memory in hydrothermal and annealed magnetites is ascribed to nucleation events above the threshold level, and the additional size-dependent AF demagnetization of memory in high-stress unannealed grains is explained by wall unpinning from strong stress centers.

Salaoru, T., *et al.*, 2004, **Reversed gyroremanent magnetization in γ-Fe_2O_3 particulate systems**: *IEEE Transactions on Magnetics, v.40*, no.4, p.2407-9.
The "normal" GRM effect was explained by Stephenson in 1980, but recently a "reversed" GRM was obtained in a CrO_2 particle system by Madsen. We have studied samples of γ-Fe_2O_3 particles (commercial magnetic recording tapes) and have identified samples with both "normal" and "reversed" GRM. The amplitude of the ac field was found to essentially influence the character of the GRM. In this paper, we also present micromagnetic simulations of the GRM in systems of single-domain particles and the results are discussed. Both "normal" and "reversed" GRM have been obtained in the simulations.

Mineral & Rock Magnetism

Carter-Stiglitz, B., Moskowitz, B. and Jackson, M., 2004, **More on the low-temperature magnetism of stable single domain magnetite: Reversibility and non-stoichiometry**: *Geophys. Res. Lett., v.31*, no.6, doi:10.1029/2003GL019155.
The loss in remanence at T_V was modeled for elongate SD magnetite for: 1) thermal cycling of RTSIRM, 300 → 10 → 300 K, and 2) warming of ZFC and FC remanences from 10 K to 300 K. Minor non-stoichiometry lowers the drop in remanence at T_V and increases the "δ ratio" (δ_{fc}/δ_{zfc}) to values as high as ~6. New experiments demonstrate that maghematization (non-stoichiometry) can partly explain the low-temperature magnetic behavior observed in magnetotactic magnetite to date.

Fukuchi, T., 2003, **Strong ferromagnetic resonance signal and magnetic susceptibility of the Nojima pseudotachylyte in Japan and their implication for coseismic electromagnetic changes**: *Journal of Geophysical Research, v.108*, no.B6, doi:10.1029/2002JB002007, correction in doi:10.1029/2003JB002648.
Magnetic susceptibilities of the Nojima pseudotachylyte are 10^2-10^3 times larger than those of the surrounding fault gouge and are proportional to the FMR signal intensities. Here I reconstruct the magnetization process of fault gouge during ancient seismic fault slip using the FMR signal. The results indicate that the instantaneous magnetization of the Nojima fault gouge may have induced instantaneous geomagnetic changes and that the instantaneous geomagnetic changes may have further induced geoelectric changes by electromagnetic induction.

Gilder, S. A., LeGoff, M., Chervin, J.-C. and Peyronneau, J., 2004, **Magnetic properties**

of single and multi-domain magnetite under pressures from 0 to 6 GPa: *Geophys. Res. Lett., v.31,* no.10, doi:10.1029/2004GL019844.
We measured the acquisition of IRM, DC demagnetization, and AF demagnetization of MD and SD magnetite under hydrostatic pressures to 6 GPa. SIRM of MD magnetite increases 2.8 times over initial values by 6 GPa, while its H_{CR} remains relatively constant. For SD magnetite, H_{CR} and SIRM vary little from 0 to 1 GPa, increase markedly from 1 to 3 GPa, then plateau above 3 GPa, suggesting a possible magnetic phase transition. Similar behavior is not observed in MD magnetite, likely due to domain wall effects.

Lagroix, F., Banerjee, S. K. and Jackson, M. J., 2004, **Magnetic properties of the Old Crow tephra: Identification of a complex iron titanium oxide mineralogy**: *J. Geophys. Res., v.109,* no.B1, doi:10.1029/2003JB002678.
Three phases of the magnetite-ulvöspinel solid solution series, $Fe_{3-x}Ti_xO_4$, x = 0, 0.1, and 0.3 are identified along with one phase of the ilmenite-hematite solid solution series, $Fe_{2-y}Ti_yO_3$, y = 0.83. Low-temperature $\chi'(f,T)$ and $\chi''(f,T)$ are found particularly useful in identifying the magnetic ordering temperature of titanohematite phases with y > 0.8 and may play an equally important role as magnetic indicator of titanomagnetite.

Yu, Y., Tauxe, L. and Moskowitz, B. M., 2004, **Temperature dependence of magnetic hysteresis**: *Geochem. Geophys. Geosyst., v.5,* no.6, doi:10.1029/2003GC000685.
For synthetic magnetite samples and gabbros, shape anisotropy dominates most temperature ranges, while magnetocrystalline anisotropy controls hysteresis properties below 120 K. Titanomagnetite-bearing oceanic basalts show quite different behavior with much higher coercivity, resulting from prominent magnetostrictive anisotropy. While many factors such as composition, field treatment, grain shape and size, and stress affect hysteresis properties at various temperature ranges, a dominant anisotropy was better recognized when remanence ratio was plotted against coercivity.

Mineral Physics & Chemistry

Berdunov, N., Murphy, S., Mariotto, G. and Shvets, I. V., 2004, **Room temperature study of a strain-induced electronic superstructure on a magnetite (111) surface**: *Physical Review B, v.70,* no.8, 085404.
A magnetite (Fe_3O_4) single-crystal (111) surface has been studied at various oxygen-iron surface stoichiometries. We have found the conditions that lead to the formation of an oxygen-rich surface that forms a quasihexagonal superstructure with a 42 A periodicity, observed by both low-energy election diffraction and scanning tunneling microscopy. We have modeled these results and calculated the electron density using density functional theory calculations, clearly showing the development of strain along the surface.

Fulde, P., 2004, **Itinerant d electrons in spinels**: *Journal of Physics: Condensed Matter, v.16,* no.11, p. S591-8.
We review a number of different approaches which have been used in order to explain the physical properties of some metallic spinels, in particular of magnetite Fe_3O_4 and LiV_2O_4. It is also pointed out that in geometrically frustrated lattices such as the pyrochlore structure one may have excitations with fractional charge.

Garcia, J. and Subias, G., 2004, **The Verwey transition-a new perspective**: *Journal of Physics: Condensed Matter, v.16,* no.7, p. R145-78.
This review puts in doubt the classical description of the Verwey (metal-insulator) transition in magnetite on the basis of the wide set of experiments carried out over the last 60 years. We re-analyse here the most relevant experiments used to study the Verwey transition from the point of view of their degree of agreement with the proposed Fe^{2+}-Fe^{3+} charge ordering model. We focus, in particular, on the results of some recent x-ray resonant scattering experiments carried out on magnetite that directly prove the lack of ionic charge ordering in such mixed valence oxide. We outline some implications for the physics of 3d transition metal oxides.

Huang, D. J., *et al.*, 2004, **Spin and orbital magnetic moments of Fe_3O_4**: *Physical Review Letters, v.93,* no.7, 077204.
New measurements of the spin and orbital magnetic moments of Fe_3O_4, using SQUID and magnetic circular dichroism in soft x-ray absorption, show that Fe_3O_4 has a noninteger spin moment, in contrast to its predicted half-metallic feature. Fe_3O_4 also exhibits a large unquenched orbital moment. Calculations using the local density approximation suggest that strong correlations and spin-orbit interaction of the 3d electrons result in the noninteger spin and large orbital moments of Fe_3O_4.

Levy, D., Artioli, G. and Dapiaggi, M., 2004, **The effect of oxidation and reduction on thermal expansion of magnetite from 298 to 1173 K at different vacuum conditions**: *Journal of Solid State Chemistry, v.177,* p. 1713-16.
Thermal expansion curves of natural and synthetic magnetite differ when measured under different vacuum conditions (10^{-4} and 10^{-6} mbar), which control the partial oxidation of the sample. If the vacuum is poor, that is in mildly oxidizing conditions, the thermal expansion curve presents a discontinuity at 875 K and the samples oxidizes. In non-oxidizing conditions the discontinuity is not present and the thermal expansion coefficient is markedly smaller. The experimental curves indicate that virtually all thermal expansion data on magnetite in the literature were measured on oxidized or partially oxidized samples.

Patermarakis, G., Papaioannou, J., Karayianni, H. and Masavetas, K., 2004, **Interpretation of electrical conductance transition of hematite in the spin-flip magnetic transition temperature range**: *Journal of the Electrochemical Society, v.151,* no.8, p. J62-8.
Impedance spectroscopy was used to investigate the electrical conductance transition and correlate it with the magnetic transition. The results suggest that the transition from antiferromagnetically to weak ferromagnetically coupled Fe^{3+} and vice versa takes place through their transformation to uncoupled Fe^{3+} and establishment of an equilibrium between these types of coupled and uncoupled pairs of Fe^{3+}. A thermodynamic model precisely predicts the dependence of magnetic transition on temperature and the appearance of peaks in both the uncoupled Fe^{3+} concentration and conductivity within the transition temperature range.

Zhou, Y., Xuesong, J., Mukovskii, Y. M. and Shvets, I. V., 2004, **Kinetics of oxidation of low-index surfaces of magnetite**: *Journal of Physics: Condensed Matter, v.16,* no.1, p.1-12.
A new technique utilizing the in situ hot stage of a high-resolution x-ray diffractometer, as well as Raman spectroscopy and vibrating sample magnetometry, show that on (111), (110) and (100) magnetite surfaces a non-epitaxial layer of haematite was formed as a result of annealing at 300°C in air. The oxidation rate for the (100) surface was significantly greater than for the other two surfaces. Parameters of the oxidation kinetics suggest that the mechanisms of oxidation for these three orientations are different.

Modeling and Theory

Carvallo, C., Muxworthy, A. R., Dunlop, D. J. and Williams, W., 2003, **Micromagnetic modeling of first-order reversal curve (FORC) diagrams for single-domain and pseudo-single-domain magnetite**: *Earth and Planetary Science Letters, v.213,* p. 375-90.
Modeled FORC diagrams show a single peak centered on Hc for individual elongated SD grains, and multiple peaks for PSD grains with vortex structure. Arrays of elongated SD model particles yield two distinct patterns depending on the spacing between particles, with a secondary branch on the reversal curves if the spacing between particles is less than about twice the particle length. This feature translates into the appearance of one negative and three positive peaks on the FORC diagram. The presence of symmetric peaks on a FORC diagram can be an indicator of the presence of either small PSD grains or magnetic interactions in an ensemble of grains.

Fukui, S., *et al.*, 2004, **Analytical study on open gradient magnetic separation using quadrupole magnetic field**: *IEEE Transactions on Applied Superconductivity, v.14,* no.2 Special Issue SI, p.1572-1575.
A numerical model to analyze the diffusion process of magnetic particles suspended in a fluid in a quadrupole magnetic field was developed based on the equation of the mass conservation. The concentration profiles of the magnetic particle are numerically obtained by using the model. The feasibility of the open gradient magnetic separation using the quadrupole magnetic field was verified by the numerical results.

Knudsen, M. F., Jacobsen, B. H. and Abrahamsen, N., 2003, **Palaeomagnetic distortion modelling and possible recovery by inversion**: *Physics of the Earth and Planetary Interiors, v.135*, no.1, p.55-73.
A robust finite-element technique for computation of both the internal demagnetization effects and magnetic terrain effects in bodies with arbitrary shape and susceptibility distribution facilitates analysis of the palaeomagnetic deflection problem. We find a systematic shallowing of inclination for bodies with a horizontal elongation. An inverse procedure for elimination of the deflection effect requires that the magnetic body is quite homogeneous and that its surface geometry is known, as may be the case for historical lava flows. When geometry is unknown and no correction applied, palaeomagnetic conclusions must take into account the possible bias from internal demagnetization and magnetic terrain effects.

Vieille, B., Buiron, N., Pellegrini, Y. P. and Billardon, R., 2004, **Modeling of the magnetoelastic behaviour of a polycrystalline ferrimagnetic material**: *Journal de Physique IV, v.115*, p.129-137.
The effect of stresses on the magnetic behaviour of polycrystalline ferrites has been investigated by the use of experiments and a multiscale model. At the scale of the magnetic domain, minimisation of energy gives the orientation of magnetisation under the effect of magnetic field, stresses, and crystal orientation. At the scale of the single crystal, the volume fractions of domains of different orientations are computed from their respective energies through a balance equation that introduces two adjusting parameters. The isotropic polycrystalline behaviour is deduced from the averaging of the behaviour of a sufficient number of grains (of different crystallographic orientations). The predictions are in good agreement with experimental results.

Synthesis and Properties of Magnetic Materials

Alcala, M. D., *et al.*, 2004, **Synthesis of nanocrystalline magnetite by mechanical alloying of iron and hematite**: *Journal of Materials Science, v.39*, no.7, p.2365-70.
The synthesis of magnetite has been studied by mechanical alloying in an inert atmosphere of a stoichiometric mixture of micrometric particle size iron and hematite powders. The final products have been characterised by chemical analysis, SEM, TEM, XRD, Mossbauer spectroscopy as well as specific surface and magnetic measurements. The magnetite obtained in this way exhibits a high magnetic hardness. The formation of a wustite layer on the magnetite core, because of the reaction between magnetite and iron contamination coming from the bowls and grinding balls, tends to decrease the coercive force of magnetite. The formation of this phase would be avoided by controlling the grinding time.

Gundiah, G., *et al.*, 2004, **Dip-pen nanolithography with magnetic Fe_2O_3 nanocrystals**: *Applied Physics Letters, v.84*, no.26, p.5341-3.
Dip-pen nanolithography has been employed to obtain magnetic nanopatterns of γ-Fe_2O_3 nanocrystals on mica and silicon substrates. The chemical and magnetic nature of the patterns have been characterized employing low-energy electron microscopy, x-ray photoemission electron microscopy, and magnetic force microscopy measurements.

Jian, X., Thompson, S., O'Keefe, E. and Perry, C. C., 2004, **Iron oxide-silica nanocomposites via sol-gel processing**: *Materials Letters, v.58*, no.11, p.1696-700.
Iron-containing silica nanocomposites were prepared via sol-gel processing using an iron-containing citrate solution. The samples were analysed via thermogravimetry, X-ray diffraction (XRD), transmission electron microscopy (TEM) and infrared (IR) spectroscopy. The effect of sintering temperature on the magnetic susceptibility of the composites was also studied.

Jeong, J.-R., Lee, S.-J., Kim, J.-D. and Shin, S.-C., 2004, **Magnetic properties of Fe_3O_4 nanoparticles encapsulated with poly(D,L lactide-Co-glycolide)**: *IEEE Transactions on Magnetics, v.40*, no.4, p.3015-17.
We have investigated the magnetic properties of Fe_3O_4 nanoparticles encapsulated with poly(D,L lactide-Co-glycolide) (PLGA) prepared by an emulsification-diffusion technique. The size of nanoparticles was reduced down to 90 nm through the optimization of the preparation condition such as homogenizer and agitator speed. Zero-field-cooled (ZFC)/field-cooled (FC) magnetization , magnetic hysteresis, and relaxation measurement were performed using a SQUID magnetometer from 5 K to 300 K. The SQUID measurements show superparamagnetism of nanoparticles with a blocking temperature of 120 K. By measuring the magnetic relaxation of the magnetization at 5 K, we obtained magnetic viscosity of PLGA-encapsulated Fe_3O_4 nanoparticles.

Liu, Z. L., *et al.*, 2004, **Synthesis of magnetite nanoparticles in W/O microemulsion**: *Journal of Materials Science, v.39*, no.7, p.2633-6.
Magnetite nanoparticles have been successfully synthesized by using a new microemulsion method. The structure and composition of particles are characterized by XRD and FTIR, which shows the sample is composed of magnetite. TEM image shows the magnetite particles have an average diameter of 10nm and in the shape of quasisphere. The magnetic measurement showed the magnetite nanoparticles have perfect superparamagnetism and high Curie temperature Tc value of 860 K. Thermogravimetric analysis (TGA) was studied in the temperature range from 493 to 923 K in an argon atmosphere. It is demonstrated that the new method provided is a very effective way to synthesize magnetite nanoparticles.

Matsunaga, T., Okamura, Y. and Tanaka, T., 2004, **Biotechnological application of nano-scale engineered bacterial magnetic particles**: *Journal of Materials Chemistry, v.14*, no.14, p.2099-2105.
Much effort has been devoted to the preparation of nano-sized magnetite particles with well-controlled size and shape. Magnetic bacteria synthesize uniform and nano-sized magnetite particles enveloped by organic lipid membranes. This review discusses recent advances in bacterial magnetite particles. Especially, the tremendous biotechnological potential of bacterial magnetite particles (BMPs) and our recent understanding of mechanism of magnetite particle formation in Magnetospirillum magneticum strain AMB-1 were highlighted.

Slawska-Waniewska, A., *et al.*, 2004, **Effect of surface modifications on magnetic coupling in Fe nanoparticle systems**: *Physical Review B, v.70*, no.5, 054412.
The correlation between structure and magnetic properties of Fe particles with core-shell structure (with the ratio of their linear dimensions of around 11:2 nm) has been investigated. In the as-prepared particles the surface layer, composed of small clusters of iron oxide, causes suppression of the exchange interactions and strong pinning of the core moments. Annealing leads to reconstruction of the surface layer and formation of big islands of good quality stoichiometric magnetite with sharp Verwey transition at 122 K. The exchange couplings between Fe particles across Fe_3O_4 interfaces are enhanced leading to long-range ferromagnetic correlations, reduction of the local anisotropy, and magnetic softening.

Vengalis, B., Sliuziene, K. and Lisauskas, V., 2004, **Growth and investigation of oxide heterostructures based on half-metallic Fe_3O_4**: *Acta Physica Polonica A, v.105*, no.6, p.659-665.
We report thin films of ferromagnetic Fe_3O_4 (magnetite) grown by a reactive magnetron sputtering at T = 300 divided by 450°C on lattice-matched MgO, and bilayer structures composed of Fe_3O_4 and underlying epitaxial films of highly conductive electron-doped In_2O_3<Sn>, $LaNiO_3$, and antiferromagnetic CoO. The prepared Fe_3O_4/MgO films and the bilayer structures demonstrated clearly defined resistance anomaly at Verwey transition point (T_V approximate to 100-120 K). Formation of high resistance interlayer was indicated between the adjacent conducting Fe_3O_4 and $LaNiO_3$ layers. However, relatively low interface resistivity of about 0.1 Omega cm(2) (at T = 300 K) was estimated for the patterned Fe_3O_4/In_2O_3(Sn) bilayer structures. Vertical electrical transport measurements revealed strong nonlinearity in the I-U dependences of the Fe_3O_4/In_2O_3<Sn> interface at $T < T_V$.

Mössbauer, Rudolph Ludwig

b. Jan 31, 1929, München

The 1961 Nobel Prize in Physics was shared by Mössbauer and Robert Hofstadter, the former for his discovery of recoilless nuclear resonance absorption of γ-radiation, and the latter for his work on electron scattering in atomic nuclei. Mössbauer began his research into nuclear resonance fluorescence as a graduate student under the guidance of Heinz Maier-Leibnitz at the Technische Hochschule München and the Max Planck Institute in Heidelberg. Contrary to expectations, Mössbauer observed a strong increase in absorption when ^{191}Ir was cooled in liquid N, and he recognized this as due to recoil-free resonance absorption. After publishing this discovery in his 1958 doctoral dissertation, Mössbauer carried out the critical next step of Doppler-shifting the γ-ray energies very slightly, and observing displacements of the sharp resonance peak related to different nuclear energy levels in the absorber.

"for his researches concerning the resonance absorption of gamma radiation and his discovery in this connection of the effect which bears his name" - 1961 Nobel citation

...Mössbauer

continued from p. 1

temperature or as an ordering temperature without additional constraints. However, for $T_B < T < T_N$ if we are able to apply a magnetic field large enough to force the particles into a magnetically stable state, we will then observe the magnetically split sextet, giving us a way to distinguish between T_B and T_N.

Figure 2 shows the same sample as in Figure 1, but this time we start at 60K with a 5.5 Tesla applied field. The spectrum is now split to a very broad sextet showing a distribution of hyperfine fields due either to non-equivalent local site symmetry, or to particle volume distribution. But we know from the broad sextet that we are still below T_N. As the temperature increases further we observe the spectra once again begin to collapse, and somewhere above 200K we will reach a paramagnetic doublet in 5.5 Tesla, and hence the true T_N.

We can observe the ordering at a given temperature by applying increasing external fields and watching how the spectra evolve from a doublet in zero field at 100K to a broad, somewhat collapsed sextet in 5.5 Tesla (Figure 3). Even though the spectra are partially collapsed, we can still fit a distribution of hyperfine fields and calculate an average value. To characterize nanomaterials with low T_N, where the blocking temperature and T_N are very close, this ability to separate them out is very useful for determining composition-dependence of T_N. A useful method of summarizing the data is to look at hyperfine field as a function of temperature for both zero and 5.5T applied field (Figure 4). The blocking temperature can be easily estimated to be around 60K (filled triangles) while the Néel temperature can be seen to be above 200K, although it is difficult to precisely calculate as it does not follow a typical Brillouin function for these nanophases. Mössbauer spectroscopy using low temperatures and applied fields is thus a powerful tool to study nanomaterial. It can take as long as a day to collect one spectrum, but if the samples and temperature and field steps are chosen well, the data can be valuable in determining the grain size and estimating the composition of iron-bearing material.

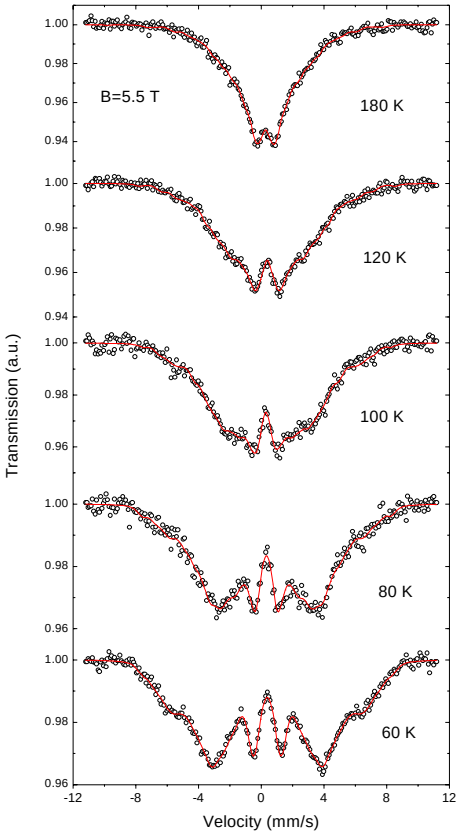

Figure 2 - Mössbauer spectra with 5.5 T applied field at different temperatures. Persistence of a collapsed sextet shows that true T_N is closer to 180K or above (not 60K).

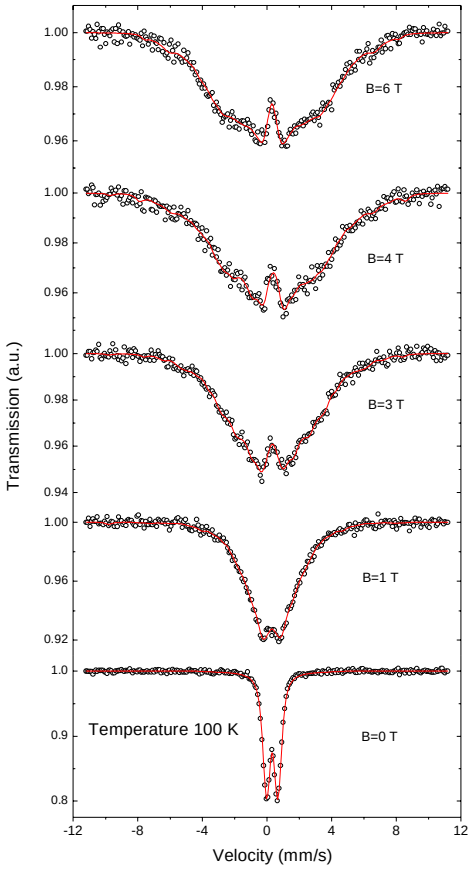

Figure 3 - Mössbauer spectra at 100 K as a function of applied field. The appearance of a collapsed sextet at 3T, and its invariance between 4 and 6T show that true T_N can be revealed, if applied field ~5T and the sample is heated to T>100K.

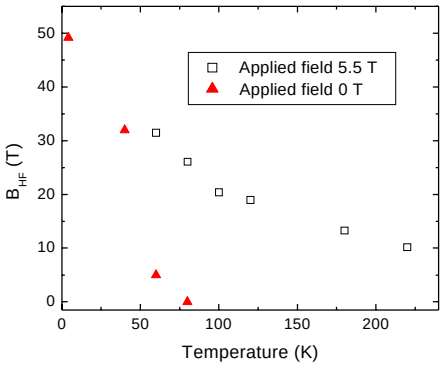

Figure 4 - Observed changes in magnetic hyperfine field (B_{HF}) with temperature and zero or 5.5 T applied field.

References

Greenwood, N. N., and Gibb, T. C. (1972), *Mossbauer Spectroscopy*, Chapman and Hall Ltd., London.

Hunt, C. P. (1992) Mössbauer: Marvelous measurements of magnetic minerals, *IRM Quarterly, 2* (3).

Muxworthy, A. (2000), Application of Mössbauer spectroscopy in environmental magnetism, *MAGazine, 2*, 6-7 <http://www.geo.uu.nl/~magnet/

Mössbauer

continued on p. 12...

The *Institute for Rock Magnetism* is dedicated to providing state-of-the-art facilities and technical expertise free of charge to any interested researcher who applies and is accepted as a Visiting Fellow. Short proposals are accepted semi-annually in spring and fall for work to be done in a 10-day period during the following half year. Shorter, less formal visits are arranged on an individual basis through the Facilities Manager.

The *IRM* staff consists of **Subir Banerjee**, Professor/Director; **Bruce Moskowitz**, Professor/Associate Director; **Jim Marvin**, Emeritus Scientist; **Mike Jackson**, Senior Scientist and Facility Manager, and **Peat Sølheid**, Senior Scientist.

Funding for the *IRM* is provided by the **National Science Foundation**, the **W. M. Keck Foundation**, and the **University of Minnesota**.

The *IRM Quarterly* is published four times a year by the staff of the *IRM*. If you or someone you know would like to be on our mailing list, if you have something you would like to contribute (*e.g.*, titles plus abstracts of papers in press), or if you have any suggestions to improve the newsletter, please notify the editor:

Mike Jackson
Institute for Rock Magnetism
University of Minnesota
291 Shepherd Laboratories
100 Union Street S. E.
Minneapolis, MN 55455-0128
phone: (612) 624-5274
fax: (612) 625-7502
e-mail: irm@umn.edu
www.irm.umn.edu

IRM

UNIVERSITY OF MINNESOTA

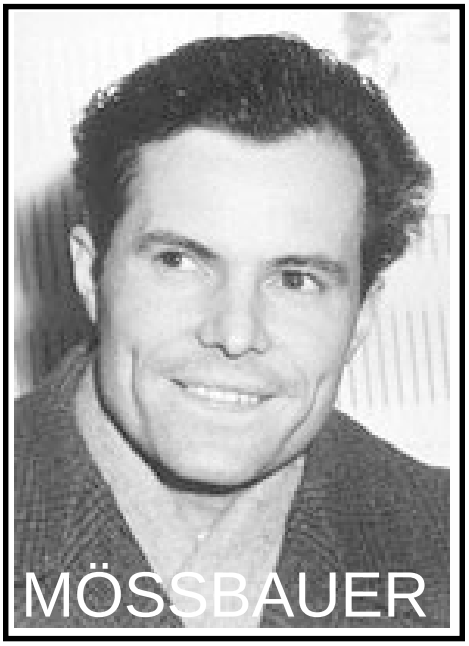

source: http://nobelprize.org/physics/laureates/1961/mossbauer-bio.html

Collector's Series #34

...Mössbauer *continued from p. 11*

MAGazine/Magazine_02.pdf>

Pankhurst, Q. A. and Pollard, R. J. (1990), Mössbauer spectra of antiferromagnetic powders in applied fields. *J. Phys.: Condens. Matter 2*, 7329-7337.

Pankhurst, Q. A. and Pollard, R. J. (1992), Structural and Magnetic properties of Ferrihydrite. *Clays Clay Miner.*, *40*, 268-272.

Sølheid, P. A. (1998) Mössbauer revisited, *IRM Quarterly*, *8* (3).

The IRM Quarterly

University of Minnesota
291 Shepherd Laboratories
100 Union Street S. E.
Minneapolis, MN 55455-0128
phone: (612) 624-5274
fax: (612) 625-7502
e-mail: irm@umn.edu
www.umn.edu